



MRI Phantom for Fat Quantification

BME 400 End of Semester Report

12/9/2009

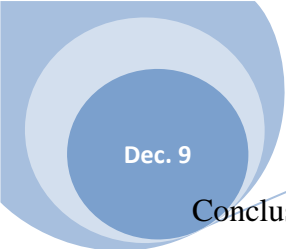
By: Matthew B Parlato, Bogdan Dzyubak, Joe Helfenberger, Nick Balge

Abstract

Fat deposits in the liver can be signs of serious health problems, and there are few accurate, non-invasive techniques that quantify liver fat. The client Dr. Scott Reeder has developed an MRI technique for hepatic fat quantification which requires a calibration device for various MR scanners. Our goal is to design an MRI phantom that represents physiologically relevant concentrations of liver fat. The phantom design includes 16 vials that contain emulsions of safflower oil and water, stabilized with crosslinked gelatin. The vials are aligned in a UHMWPE vial holder and submerged in deionized water. Testing with the client's technique has revealed that soap and formalin do not significantly affect measured fat concentrations, but differing gelatin concentrations significantly decrease the perceived fat concentration. For this reason, future emulsions should contain consistent amounts of gelatin. Vertical density testing also showed that density changed with sample depth; this must be corrected for to ensure homogeneous samples. Further testing must also ensure that the phantom is designed to last for 3 years without degradation.

Table of Contents

Abstract.....	1
Introduction.....	4
Motivation.....	4
Competition.....	5
Preliminary Design.....	6
Background.....	6
MRI Basics.....	6
IDEAL.....	8
Emulsions.....	8
Design Requirements.....	9
Client Requirements.....	9
Design Criteria.....	9
Ergonomics.....	11
Design Decisions.....	12
Structural.....	12
Component Sizes.....	12
Mechanical Materials.....	13
Chemical Decisions.....	14
Emulsion Materials.....	14
Emulsions: Selection of Oil/Water Ratios.....	15
Methods.....	16
Mechanical Construction.....	16
Emulsion Preparation.....	16
Final Prototype Design.....	17
General Structure.....	17
Testing.....	19
Testing Procedure.....	19
Results and Discussion.....	20
Testing Results and Discussion.....	21
Future Work.....	23



Conclusion 24

Bibliography 25

Appendix A – Product Design Specifications 29

Appendix B – Relevant Figures 32

Appendix C – Weight Limit Calculations 34

Introduction

In a typical, healthy liver, one would find no fat deposits. A small amount of fat is not harmful; however, large accumulations impede function. This condition, known as fatty liver disease, usually has no early warning symptoms. The most common way of diagnosing it clinically is surgical biopsy. Some non-invasive diagnosis techniques, such as the MRI two-point Dixon method, do exist, but they have limited reliability and are not widely used in clinical practice (Song, et al. n.d.). The client, Dr. Scott Reeder of the UW-Madison Radiology Department, has developed an MRI procedure (known as IDEAL) that is able to non-invasively quantify the amount of fat within a liver. However, because quantification of fat with MRI is not widespread, there exists no standard method to calibrate the technique.

This semester, a phantom was designed to calibrate the IDEAL technique to produce consistent results when used at different institutions. It contains glass vials housing oil/water emulsions, which represent relevant concentrations of hepatic fat. These vials are held in place within a horizontally oriented vial holder. This entire apparatus is then submerged in water, within a small, polypropylene tank. Because of its size and weight, it can be used, transported, and stored by one person. These dimensions are also less than that of a standard, 1-channel MRI head coil so that it may be used within one if enhanced image quality is desired. The mechanical parts of the phantom have been constructed and the procedure for making the fat samples has been developed.

Motivation

Non-alcoholic fatty liver disease (NAFLD) affects approximately 20% of the general population and covers a wide spectrum of hepatic fat accumulation, ranging from simple fatty liver disease to non-alcoholic steatohepatitis (Diamond, Thava and Scott 2003). Lipid retention in hepatocytes (steatosis) occurs in successive stages, beginning with the formation of small fat vacuoles or liposomes around the nucleus (Yoneda, et al. 2007). As the vacuoles coalesce and grow in size, the formation of permanent, fatty cysts begins (Diehl and Tetre 2006). No single mechanism leading to steatosis exists; rather a variety of pathologies disrupt normal lipid movement through the cell.

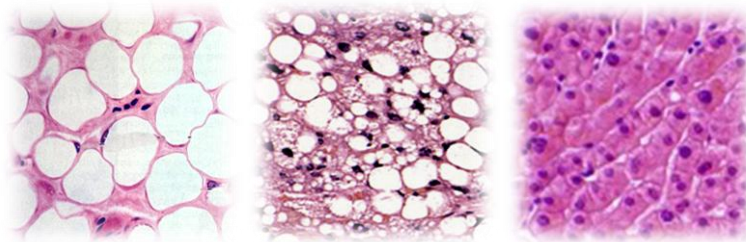


Figure 1. Images showing adipose tissue, steatotic liver cells, and normal liver cells (from left to right). Photos are from Wikimedia, and Hartnell Community college (Wikimedia: Non-alcoholic fatty liver disease1 2009) (Edens n.d.) (Wikimedia: Human Liver 2006).

Non-alcoholic steatohepatitis (NASH) occurs when hepatic fat accumulates enough to cause tissue damage. Affecting 2.5% of Americans, it is associated with metabolic syndrome, fat distribution, obesity, and hereditary factors (Patrick 2002). The excessive accumulation of fat in the liver prevents cellular transport of nutrients and oxygen, leading to tissue damage and inflammation (Diehl and Tetre 2006). If this tissue damage is allowed to continue, NASH progresses into severe liver scarring or cirrhosis.

The gold standard for diagnosing NASH is a liver biopsy; tissue examination definitively confirms hepatocyte damage with the presence of fat (Ferenci, Tozun and Avsar 2003). As a biopsy is invasive, alternative methods to help diagnose fatty liver are needed. Blood tests for elevated levels of alanine aminotransferase (ALT) or aspartate aminotransferase (AST) show general liver damage but lack information about fat presence (WebMD 2008). Studies of MRI techniques do show fat-presence, and additional studies have demonstrated that the fat-water ratio and steatosis grade are highly correlated ($R = 0.852$, $P < 0.0001$) (Mennesson, et al. 2009).

Current obesity trends indicate that 40 percent of the U.S. population will be obese by the year 2025. (Pessayre, et al. 2001) The incidence of diabetes mellitus is also predicted to extend to affect 7.2 percent of the US population by 2050 (Marchesini and Forlani 2002). As these trends are intimately correlated with NAFLD and NASH, a significant increase in diseased and inflamed livers is expected in the next 25 years. By developing better MRI imaging techniques, the diagnosis of NAFLD and NASH can be improved.

The client, Dr. Scott Reeder, has developed a non-invasive MRI technique to quantify the amount of fat in the liver. We seek to provide the client with a phantom to standardize MRI fat quantification procedures at various institutions. This will allow hospitals to reliably use Dr. Reeder's MRI technique to assist in the diagnosis of fatty liver disease and NASH.

Competition

There are no current phantoms that are being sold on the market for fat quantification. Several research phantoms have been built to mimic fat deposits of specific quantities in the liver. A phantom developed by Chang, *et al.* to quantify fat using opposed-phase imaging and $^1\text{H-MR}$ had used vegetable canola oil and fresh calf liver, blended and imaged in the liquid phase (2006). This demonstrated an accurate correlation between measured and known values with an R^2 values between 0.9216 and 0.9801. Another research phantom was built using a neutral triglyceride, water and an emulsifier and was analyzed using a modified Dixon method (Matsunaga, et al. 2006). Another phantom simulated the T1 and T2 of the liver using agarose gel doped with Gd-DPTA (Hannesson, et al. 1995). The first two phantoms were not intended for long term use as fat-water emulsions will separate over long periods of time. Also, the use of liver tissue cannot be used for long term phantoms. The phantom that employed doped gel represents a long term solution to a liver phantom. However, this phantom could not be used with IDEAL as the simulated materials would not exhibit the differences in spin frequencies that fat and water exhibit and were only used to simulate T1 and T2.

Preliminary Design

Pre-existing techniques have been implemented to simulate the MRI signal of hepatic fat. One utilizes droplets of animal fat suspended in water. Another technique includes pouring a layer of fat on top of a layer of water; when imaged diagonally across the two samples, the fraction of fat in water changes across the image (Reeder, Project Meeting 2009). It is also possible to construct a phantom out of materials that have similar MR properties to that of fatty liver tissue (Blechinger, Madsen and Frank 1988). Such a design opens many possibilities as materials that may be used in the phantom do not necessarily have to be naturally found in the body. As long as they mimic a fatty liver's MR signal, they are appropriate to use.

The design that we propose is one that uses oil-in-water emulsions to represent fat deposits within the liver. Such a design has the advantage of not requiring the use of animal fat or biological tissues which present degradation and sanitation concerns. Also, dispersing the oil particles homogenously throughout a solution rather than clumping them in one area will lead to greater accuracy because the signal will not depend on the imaging plane. Spatially, it is also more physiologically accurate (Albright and Stern 1998). Finally, a number of oils exist that are chemically similar to animal fat and would mimic a wide range of properties.

Background

MRI Basics

MRI is nearly ubiquitous in modern medicine. This technique uses strong magnetic fields and radio-frequencies to generate images of tissues. MRI is non-invasive and does not have the radiation concerns that X-ray based techniques do. Indeed, MRI has not been shown to produce harmful effects in any person or developing fetus (Koka, et al. 2004). The fact that MRI is safe and can produce excellent pictures of soft tissue has allowed it to become a common medical imaging method.

The theory behind how an MRI machine works is based on a particle property called spin. Atoms such as hydrogen that have an odd number of particles in their nucleus have a net spin. Atoms with an even number of particles in the nucleus, such as carbon, have a spin of zero. An MRI machine takes advantage of this property by aligning the spins of all particles in the body (primarily hydrogen) in the same direction by applying a strong magnetic field on the order of 1.5 – 3 T. Applying additional electromagnetic waves at proper frequencies (in the radiowave range) will cause certain spins to absorb the energy and enter a high energy state in which they are aligned directly against the magnetic field. Eventually, the spins decay back to the low energy state reemitting the radiowaves. The period of time that it takes for the spins to decay depends on the chemical environment the atoms are in. It is called the T1 relaxation time and is one of the ways of providing contrast in MRI images. T2 and T2* relaxation times are the other two common methods and rely on similar principles. The position of the signal is determined from two factors. Additional two magnetic field gradients are applied in directions perpendicular

to the main field and to each other. The resonant frequency at which hydrogen spins absorb energy is:

$$\text{Resonant frequency} = 42.58 \times B$$

where B is the local magnetic field. Thus, only one line in the 3 dimensional space of the object being scanned experiences the same magnetic field and will absorb a given frequency. The other gradient causes every spin in the line to precess around its axis at a different rate. Thus, over time, all the spins acquire a phase difference and the exact position along this 1 dimensional line can be determined.

Because most elements except hydrogen have no spin, only materials containing hydrogen are visible on MRI. The human body is largely water so it is easily visible. Moreover, the great variety of chemical environments in which hydrogen is present in the body provides a great deal of contrast. When building an MRI phantom it is desirable to either have the structural components invisible, in which case plastics are used, or have them resemble the body, which is achieved by using water. Certain materials, though invisible themselves, can influence and distort MRI images. A very important example of this is oxygen. While it has no net spin and is invisible on MRI, oxygen possesses paramagnetic properties. When subjected to a strong magnetic field, it creates an opposing field. This distorts the signal attained from visible objects. Thus, air interfaces should be avoided when building MRI phantoms. Iron, aside from the dangers associated with placing a large magnetic object near a strong magnetic field, can distort the signal when present in small quantities, such as the amount in the liver.

As with any process, there are many factors that can affect the final outcome. One of particular importance to this project is that of signal density. Density is, of course, the mass of a substance divided by its volume; signal density is an analogue of sorts defined as:

$$\text{Signal Density} = (\text{Amount of Signal Produced}) \div (\text{Volume Producing that Signal})$$

$$\frac{\text{Amount of Signal}}{\text{Gram of Material}} \times \frac{\text{Grams of Material}}{\text{Volume Material Occupies}} = \frac{\text{Amount of Signal}}{\text{Volume Material Occupies}}$$

Thus, an MR image containing 50% water and 50% fat shows that the sample is half water half fat by density. In a given volume, this relationship refers to a mass fraction of fat and water. So, fat fractions to be quantified with MRI should be made as mass fractions. Alternatively, a correction factor may be applied.

IDEAL

The client's fat quantification technique is based on the principle of phase shifts. The behavior of the spins of hydrogens in different chemical environments varies. Among other things, the rate of precession (rotation of the spin around its axis) in a magnetic field, similar to the movement of an electron in a circle within a magnetic field, depends on the chemical environment. Thus, hydrogens in fat and water precess at different rates. Over time, they acquire a phase difference. An earlier technique, called the 2 point Dixon method uses this effect by acquiring two images, one with fat and water in phase and one with them out of phase (Heiken, Lee and and Dixon 1985). The two images are added resulting in the water signal doubling and the fat signal canceling itself out. This yields a water-only image. Then, the images are subtracted yielding a fat-only image. The two images are used to calculate the fat fraction. Unfortunately, in actuality the magnetic field experienced by the object being imaged is changed by the object itself to an extent that is difficult to predict. This causes the precessions to occur at rates different from the predicted ones and makes the fat-water separation less accurate. The main difference in the IDEAL technique is that it uses 3 phase images, instead of 2, to evaluate the magnetic field deviation as well as the water-only and fat-only images. This and other improvements make the technique significantly more accurate for real-world applications.

Emulsions

Due to the simultaneous presence of water and fat in the liver, a mixture of fat and water is a logical possibility for the simulation of fatty liver. However, the polarity of water molecules and triglycerides present a challenge in creating a homogeneous mixture. The addition of an emulsifier will allow the non-polar lipids to intersperse between the polar water molecules.

Emulsifiers work to counteract the intermolecular repulsive forces between the polar water molecules and non-polar oil molecules. The molecules of the emulsifier have both polar and non-polar ends. In an aqueous solution, emulsifier molecules aggregate into spheres called micelles with their non-polar ends facing inwards and polar ends facing outwards. Non-polar fat molecules then become trapped within the micelles and are able to be dispersed throughout the mixture.

Over a long period of time, even a well-made emulsion will begin to separate. This is due to the differing densities of oil and water; oil (being less dense than water) will eventually float to the top of the mixture. To prevent this, a stabilizer must be used to compartmentalize the dispersion.

Two types of stabilizers exist, and each works on a different basis. Liquid phase stabilizers slow separation by increasing the viscosity of a liquid to the point where flow is very slow. Solid phase stabilizers work by creating a cross-linked matrix that literally traps the components in place. Separation occurs only due to leakage through the matrix and is extremely slow.

Design Requirements

Client Requirements

First and foremost, the client requires that the phantom be completely MRI compatible. This means that no metal components, no magnetic components, nor any other materials that are known to interfere with MRI procedures be used. Obviously, the phantom must also fit within a standard MRI machine. Furthermore, it is possible that additional transmitter-receiver coils may be used with this phantom; therefore, the phantom must fit within these, as well. It should also be noted that this phantom will be placed into an MRI machine that patients are also placed into. It follows from this that the phantom should contain no extremely toxic components that, if spilled onto the MRI machine, could harm a patient.

The client's IDEAL procedure utilizes a voxel size of 1.3 X 1.8 X 10 mm (0.051 X 0.071 X 0.315 in) (Reeder, Personal Communication 2009). The client also desired to have at least 10 voxels across one sample. All vials should also be oriented parallel to the main magnetic field of the MRI as this will limit magnetic field inhomogeneity around the vials (Schenck 1996) (Reeder, Personal Communication 2009).

As the main purpose of this phantom will be the calibration of the IDEAL procedure, it must contain realistic fat concentrations. Several fat concentrations of around 5% fat should be represented as this is the diagnostic cutoff for fatty liver disease (Reeder, Personal Communication 2009). Fat concentrations in the liver have typically fallen between 0% and 30% in the client's experience, but concentrations as high as 50% have been observed so it is important that this entire range is incorporated into the phantom (Reeder, Personal Communication 2009). Adipose tissue may also be quantified with this technique (Reeder, Project Meeting 2009), so it is important that at least a few samples simulating the fat concentration of adipose tissue are included, as well. Adipose tissue is composed of approximately 60% to 95% fat (Albright and Stern 1998).

It is also required by the client that the MRI signal of the phantom be constant over time. All results obtained from it with the IDEAL procedure must be repeatable and accurate to within $\pm 0.3\%$ (Block and Hines 2009). A useful lifetime of between 3 and 5 years is also desired (Reeder, Project Meeting 2009).

Design Criteria

Most importantly, since the phantom will be imaged using a strong magnetic field, it should contain no magnetic materials. Ferromagnetic materials, such as iron, must be avoided as they would compromise safety. Other materials possess non-negligible magnetic properties and can interfere with the imaging. These materials include but are not limited to:

1. **Air** – Oxygen has paramagnetic properties (in the presence of a magnetic field it creates an opposing magnetic field). This can have significant

influence on the perceived position of objects in the image. Air inside and around the phantom should thus be avoided.

2. **Impurities in Water** – Impurities in many water sources consist of metal ions that could potentially interfere with the MR imaging.
3. **Metallic Impurities in Glass** – Some types of glass, especially colored glass, contain ferromagnetic metal impurities that will interfere with MRI imaging.

The voxel sizes employed by the IDEAL procedure, along with specific requests by the client, restrict sample sizes to a minimum of 9 mm (0.35 in) across, and preferably 18 mm (0.7 in). The samples will be separated by 12.7 mm (0.5 in), which corresponds to 7 pixels. This will keep the signal of one vial from interfering significantly with the signals of its neighbors (Block and Hines 2009). Samples near the outside of the phantom will be 3.5 pixels (6.35 mm or 0.25 in). This will allow one to easily distinguish the edge of the sample from random background noise.

Although the client's fat quantification technique is primarily intended for the liver, it may be useful to use the phantom to mimic other regions of the body using different fat concentrations. The imaging of some other body parts requires additional transmitter-receiver coils that are placed around the patient inside the scanner. The 1-channel head coil is the smallest one that would be used for such measurements. It is 10.63 in diameter by 17.7 in deep. The phantom should completely fit into this coil.

As the phantom's purpose is to calibrate MR fat quantification measurements, it is necessary that all oil/water emulsions are accurate. In addition, the primary region of interest is around 5% fat so many oil/water emulsions should be focused around this region. As the client has indicated that fat fractions above 30% are rare, only a few samples above this concentration should be included. One or two samples of very high fat fractions (90% fat or greater) should be included as a reference in cases where adipose tissue is present in the image. A sample of 0% fat and 100% fat will also be included as reference points.

Due to the different densities of oil and water, MR signal density will be of great concern. To overcome this problem, all emulsions will be measured by weight rather than by volume. This will compensate for the fact that oil and water have such different densities. Care must also be taken that sample densities are constant throughout their bulk as varying densities of the samples may also lead to differing signal densities.

All IDEAL procedure results must be repeatable and accurate. Therefore, extensive testing of the phantom must be conducted to ensure that all results obtained from it are indeed repeatable and accurate to the client specification of $\pm 0.3\%$. A standard procedure for use of this phantom should be developed to help ensure this repeatability and accuracy. All samples within this

phantom should also be held parallel to the main magnetic field to reduce error from magnetic field inhomogeneity, and the samples should be submerged in deionized water to reduce noise associated air-to-sample interfaces.

The client intends to use the phantom for a number of years; therefore, any components used to build it must be long lasting. The phantom should maintain structure as well as function over a period of at least 3 years, meaning that the signal obtained from imaging the fat fractions must be consistent over time. Animal fat degrades over a period of months, depending on which preservatives are used making it unsuitable for use in this phantom. Preservatives that significantly slow this degradation may be quite toxic and the client has specifically requested that no extremely toxic substances be used in this phantom. Plant oils, however, are composed of very similar organic acids to that of human fat (Christie 2009), but do not suffer from the same degradation concerns. Therefore, plant oils will be used in this phantom instead of animal fat. Steps should also be taken to avoid microbial degradation of other natural biomaterials used in the emulsions.

Ergonomics

Two main considerations should be taken into account throughout the design process. As mentioned in the general Design Criteria, the weight of the prototype should be minimized to avoid any physical strain caused to the tester. Weight limit guidelines obtained from the US Department of Labor can be seen in Appendix C. The phantom weight has been limited to less than 20 lb which satisfies these requirements.

Design Decisions

Structural

Component Sizes

The components of our final design were chosen based our design constraints. To reduce interference, the phantom will be submerged in water which requires some type of outer casing. Inside the outer casing, vials will be aligned along the bore of the magnetic field in a vial holder to reduce inhomogeneity.

The 1-channel MRI head coil that our phantom should fit in has a diameter of 10.63 inches which limits the phantom's total size.

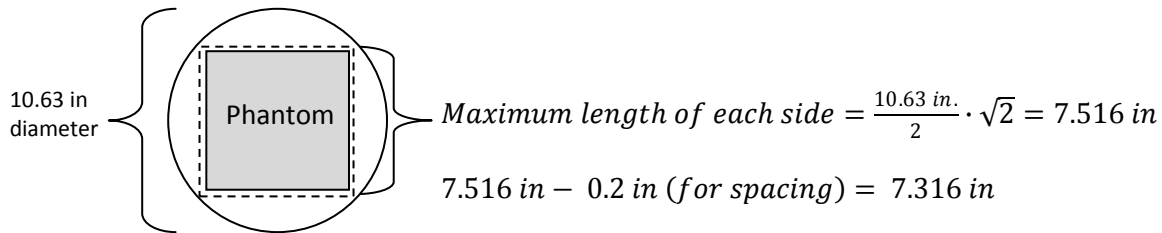


Figure 2: A diagram of the phantom in the 1-channel head coil, looking down the bore of the magnetic field.

The inner vial holder will be smaller than the outer casing to allow for casing thickness and spacing. Thickness of the outer casing is taken to be 0.5 in and necessary top/side spacing is 0.25 in on either side. This requires that $(0.5 \text{ in}) \cdot 2 + (0.25 \text{ in}) \cdot 2 = 1.3 \text{ in}$ are subtracted when assessing the vial holder dimensions.

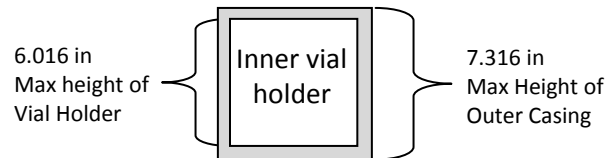


Figure 3: Dimensions of the vial holder (inner box) and the outer casing (outer box).

A vial holder of 6 x 6 inches was chosen in order to fit into the head coil.

The vial size constraints are determined by voxel size. A vial that contains 12 usable voxels across the sample was chosen.

$$\frac{0.82 \text{ in (Inner diameter)}}{0.0512 \frac{\text{in}}{\text{voxel}}} - 4 \text{ voxels (edge interference)} = 12.4 \text{ voxels}$$

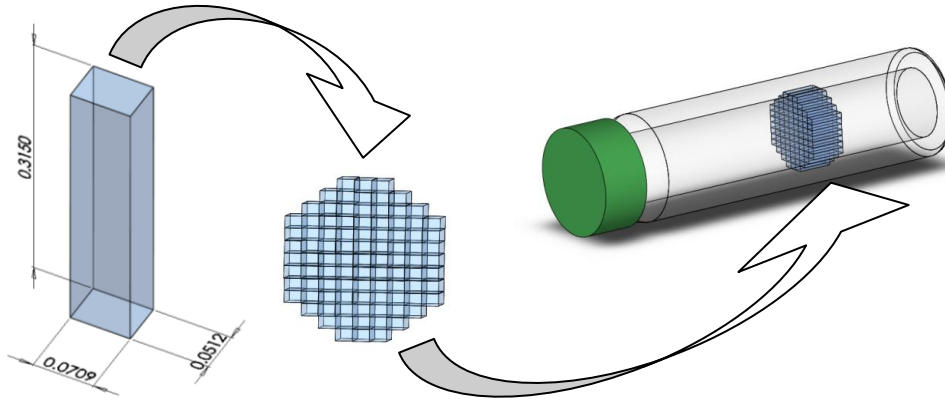


Figure 4: Diagram of the voxels dimensions that must fit inside the selected vial size.

The inner diameter of the vial is 0.82 inches, with an outer diameter of 0.97 inches, making the hole that must be drilled on the vial holder 1 inch.

The possible vial conformations are shown below in Figure 5, the 5 x 5 or a 4 x 4 setup. The 4x4 setup was chosen as 16 vials was enough to encompass physiological relevant fat values, and the 0.5 inch separation between vials in 4x4 setup was preferable to the 0.2 inch separation in 5x5, both for machining purposes and MRI interference.

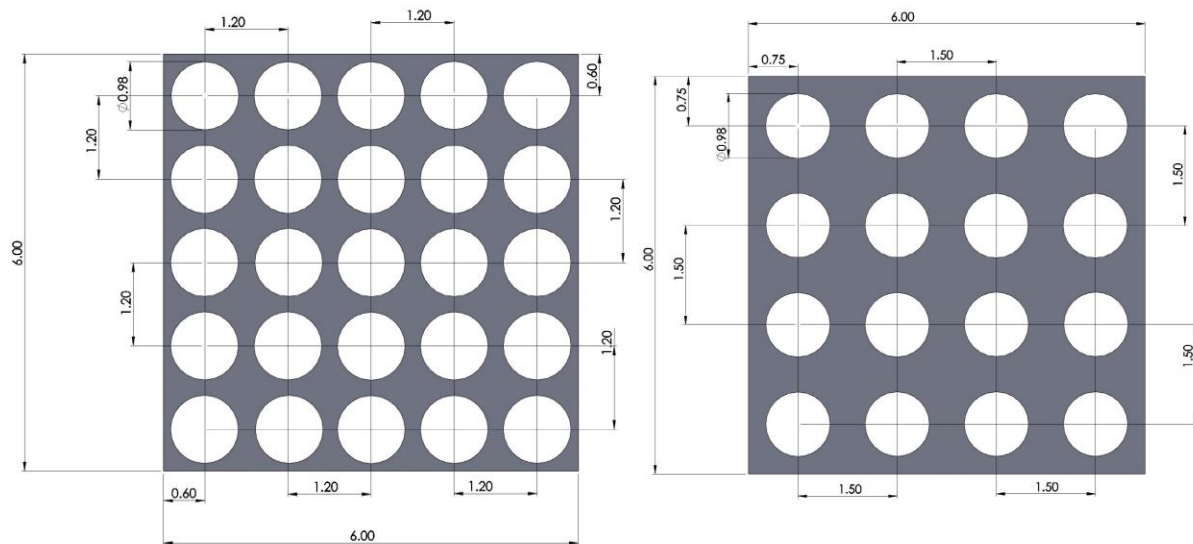


Figure 5: Diagram of a 5x5 and 4x4 vial conformation. The 4x4 conformation was chosen for our phantom.

Mechanical Materials

The vials holder was chosen to be made out of UHMWPE for its machinability, price, and lack of water retention. For a 4 x 6 x 6 block of UHMWPE, its price was 23% less expensive than the closest alternative plastic, Nylon (Plastics 2009). In addition, UHMWPE absorbs the least amount of water after 24 hours and at saturation point for feasible plastics. UHMWPE also complies with FDA standards.

Table 1: Relevant information for selection of the vial holder plastic. The machinability of each polymer on this list was classified as similarly easy for drilling purposes (**Boedecker 2009**).

	Price (Plastics 2009)	Designed to be washed regularly? (Plastics 2009)	Regulation Compliance (Plastics 2009)	Water Absorption (Gerbig 2009)
UHMWPE	\$43.75 for 6x6 block	Yes	FDA, ASTM, USDA, 3A	0.01 wt % in 24 h 0.01 wt % saturation
Nylon	\$53.70 for 6x6 block	Yes	FDA, 3A, ASTM, UL	0.25 – 1.2 wt% in 24 h 6.5-9.0 wt % at saturation
Acetal	\$282.88 for 12x12 (\$70.5 for each 6x6 block from this)	Yes	FDA, USDA, NSF, UL, ASTM, 3A	0.25 wt % in 24 h 0.9 wt % saturation
Chemically Resistant PVC	\$363.18 for 12x12 (\$90.75 for each 6x6 block from this)	No	UL	0.1 wt% in 24 h 0.1 wt% saturation

The outer casing was chosen to be purchased as a premade box with a watertight seal, in order to reduce production error and cost. A 6.5" x 9.2" x 3.7" polypropylene Lock and Lock® box was chosen that had a price 30% less than the polypropylene sheets we would need to make our own box (Plastics 2009).

Chemical Decisions

Emulsion Materials

In order to stabilize the mixture of oil and water, consideration was given to commonly available stabilizers, notably agar and gelatin. Agar is a high molecular weight polysaccharide derived from red-purple marine algae used as a growing medium and as a separating medium during electrophoresis. It solidifies when increased hydrogen bonding takes place at a low enough temperature (Porath and Janson 1976). Gelatin is derived from hydrolyzed collagen fibers and forms a gel when sections of its triple helix reform in the presence of water (Belechinger, Madsen and Frank 1988). The follow table summarizes pertinent information that will be used in gel.

Table 2: Matrix of relevant information for choosing gelatin or agar (**Bao, Yang and Mao 2008**) (**Mott 2005**).

	Price	Crosslinking	Melting Temp
Agar	\$0.40/g for 100 g powder. (Sigma-Aldrich 2009)	No common method	85 degrees C
Gelatin	\$0.27/g for 100 g powder. (VWR International 2009)	Aldehyde crosslinking forms covalent bonds	35 degrees C

The low temperature that gelatin melts at is undesirable, but it was chosen over agar due to its ability to be easily crosslinked by an aldehyde such as formaldehyde. This gives the gel additional strength and durability in the long run.

Sodium azide was included as a preservative due to its availability for this project and biostatic properties (SAFC 2009). Formalin was used as a commonly available aldehyde that can cross-link the amine groups on gelatin (Fraenkel-Conrat and Mecham 1948).

The oil chosen to represent human fat was safflower oil which is used in current research phantoms that contain oil dispersions. It is composed of primarily linoleic acid (Erasmus 2009), which is typically present in human fat at a concentration of 10% (Kokatmur, et al. 1979). Some other major components of safflower oil are oleic acid and stearic acid (Erasmus 2009). Both of these acids are present in human fat, as well (Kokatmur, et al. 1979). Though not mimicking the concentrations of human fat exactly, safflower oil's main components are all major components in human fat and it will be sufficient for the frequency shifts performed in IDEAL.

Safflower oil also has other advantages of being cheap, readily available, and non-toxic. Commonly used in cooking, it can be obtained from health food stores and many department stores. For instance, one gallon of safflower oil may be purchased from Amazon.com for \$36.58. Extremely pure safflower oil is not required as small variations of the fatty acid compositions from one batch of safflower oil to the next will not be easily detected by the IDEAL procedure (Block and Hines 2009), so obtaining high-grade safflower oil from chemical supply companies will not be necessary. Safflower oil has also been used extensively in other medical imaging phantoms so much literature exists about its behavior in other phantoms.

Emulsions: Selection of Oil/Water Ratios

The 16 physiological fat concentrations were selected primarily around the 5% cutoff value for fatty liver disease, including a range up to 50%. Seven of the 16 oil-to-water fractions surround 5%; Six concentrations span from 10% to 50%. This decision was made because concentrations of up to 30% fat are not uncommon, and 50% is the maximum that has been clinically observed. Three fat fractions at 90%, 92.5%, and 95% were also included to represent the fat concentration found in adipose tissue. This will serve as a reference in case regions of adipose tissue are scanned during a liver scan. The distribution of all 16 samples can be seen in Appendix B – Relevant Figures, Table 5.

Methods

Mechanical Construction

The polypropylene box required no mechanical modification before serving as the outer casing for the phantom. Similarly, the glass vials did not need to be modified prior to being used in the design. The UHMWPE block, however, required processing before being able to function as the vial holder.

A 1" bit was used to drill the 16 "vial-holding" holes into the 6" X 6" face of the block according to the spacing described above and seen in Figure 6. All holes were drilled to a depth of 3".

Subsequently, a 5/32" bit was used to implement the "air-releasing" holes. These holes were drilled from the bottom of each "vial-holding" hole through the remaining 1" depth of the block. All holes were smoothed with a deburring tool, and the block was washed with soap and water to remove dirt and shavings.

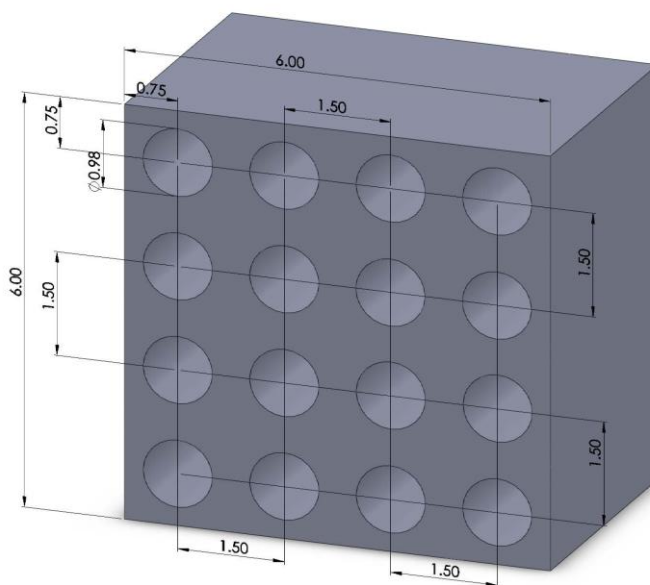


Figure 6: Diagram of the vial holder with dimensions given in inches.

Emulsion Preparation

The process developed to create the emulsions serves to standardize the amounts and techniques.

First, the desired total volume and percent fat of the emulsion are entered into a spreadsheet which automatically calculates the necessary amount of each component. This spreadsheet can be seen in Appendix B – Relevant Figures, Table 5.

The emulsion-making process, the vessels containing deionized water, gelatin, soap, and oil were massed before and after delivery. Formalin and sodium azide were made readily available but were not measured ahead of time due to their toxicity. The water was weighed into a 125 mL Erlenmeyer flask for convenience of mixing and heating.

After deionized water was massed, it was heated slowly with a magnetic stir bar. As the water began to heat, gelatin was added (Figure 7). Gelatin remaining in the weigh boat was massed again to determine the exact amount of gelatin used in the emulsion. A small piece of aluminum foil was weighed and then placed over the mouth of the flask to prevent water loss as the mixture reaches higher temperatures.



Figure 7: Addition of Gelatin.

When the mixture has reached a temperature of 150-200 degrees Fahrenheit, the oil, soap, and sodium azide was added. Soap was measured and added with a syringe for convenience. Great care should be taken to accurately weigh the oil vessel post delivery. The color should have become a slightly lighter shade.

After the addition of oil, soap, and sodium azide, the mixture was allowed to cool to room temperature. As the mixture cooled to between 100 and 120 degrees Fahrenheit, formalin was added with a calibrated micropipette. The mixture was then allowed to cool to 85 degrees Fahrenheit and was poured into a vial where it solidified. A final weight measurement must also be recorded for the foil lid. This will account for water that has condensed onto the lid after leaving the mixture.

Final Prototype Design

General Structure

The general structure of the phantom can be broken down into four parts:

- 1. Outer Case** – This is constructed of acrylic and houses the entire phantom. It also serves as a means to protect the phantom from damage during storage and use. This is filled with water and all other phantom components are submerged in this water. The outer case is currently being shipped and can be seen in Figure 8.
- 2. Vial Holder** – Constructed from ultra high molecular weight polyethylene, this will serve as a means to hold all of the vials containing the oil/water emulsions in place. It will hold all of the vials parallel to the main magnetic field to minimize distortions due to inhomogeneity in the magnetic field.
- 3. Vials** – The vials themselves are also an important part of the phantom's general structure. They will contain the oil/water emulsions and placed into the vial holder. The vials consist of pure glass with no additives that can interfere with the signal.



Figure 8: Image of Lock and Lock box used for the outer case of the phantom. This particular box was purchased from Amazon.com. (Amazon.com 2009).

4. **Emulsions** – For the final design, emulsions will be created according to the above process at each of the desired concentrations. This set will consist of 16 emulsions, completely filling the vial holder.

A projected model of the final prototype can be seen below in Figure 9.

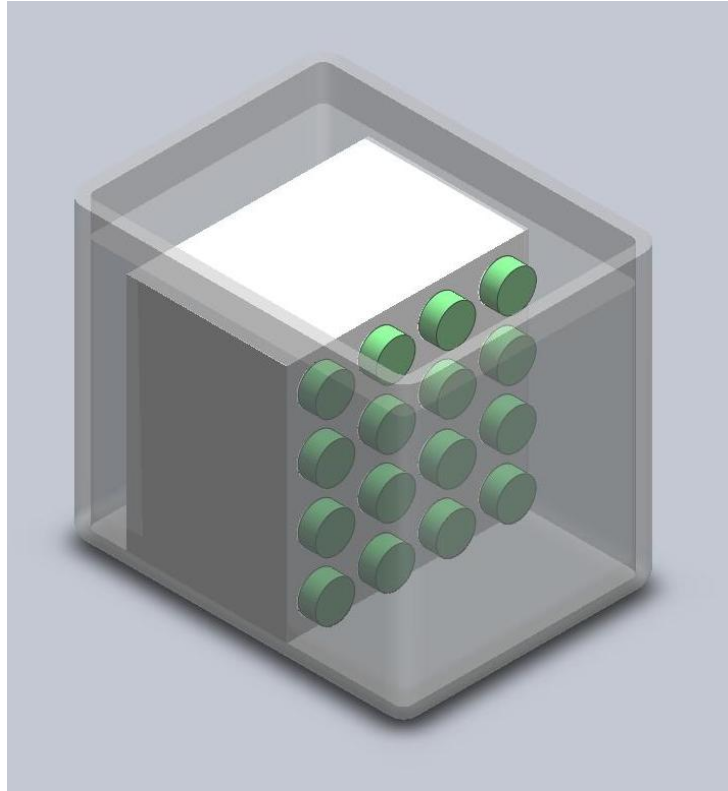


Figure 9: Projected final design.

Testing

Testing Procedure

The final product for this semester is the procedure for making fat-water samples as much as it is a number of finished samples and the mechanical structure. While making the samples, different amounts of auxiliary components (gelatin, formalin, and emulsifier) as well as different temperatures were investigated. As a result, we have determined an optimal procedure for making subsequent samples. The stability of the solid-phase emulsion was dependent on the amount of gelatin, formalin and oil as well as temperature and time allowed for cross-linking. Some emulsions separated over time if not enough gelatin had been used, and others had solidified before they could be poured into the vials when too much was used. Similarly, an excessive amount of formalin caused the gelatin to solidify within 3 seconds at temperatures as high as 170 F. An insufficient amount of soap caused incomplete emulsification, while an excessive amount may interfere with imaging. Overly low and high temperatures resulted in immediate or poor fixation. The optimal procedure that yielded well emulsified and fixated samples is presented in the results section.

Four such samples had been created successfully; their fat fractions are: 3.76%, 4.82%, 7.56%, 17.08%. An additional four samples were made specifically for testing. Due to the supply shipment being delayed, these last four were made without gelatin. One reference fraction contained 0% fat (pure deionized water) while the other 100% fat (pure safflower oil). These will be re-made once gelatin is available; however, some conclusions can be drawn. Another test sample also contained 100% fat as well as the same amount of soap and formalin used to prepare actual samples, to see how these substances affect the MRI signal. Finally, a 15% fraction was made with soap and formalin but without gelatin. This samples was compared to the fixated 15% sample to determine the effects of gelatin on the signal.



Figure 10: IDEAL Testing setup

The four fixated samples, as well as the four test samples, were scanned and quantified using the IDEAL sequence on a 1.5 T MRI scanner. This setup can be seen in Figure 10. A 1-channel headcoil was also used to gain better signal for this first test. The cross-sectional images taken half-way up the vial were analyzed (Figure 11). The imaging plane is 8 mm deep meaning that the signal is averaged over an 8 mm thick cross section. The output of IDEAL is an image with each pixel's intensity corresponding to the perceived fat fraction.

ImageJ was used to analyze the images. To calculate the fat fraction corresponding to each vial, the signal within it was averaged, except for the outer ring that is two pixels thick. These pixels were discarded due to the high level of noise at the edges.

Additionally, the samples were tested for homogeneity. When making the samples, an excess amount of gelatinized emulsions was created. These additional samples were cut horizontally into 1 cm thick disks. The densities of the disks were calculated by weighing them and measuring their dimensions. A plot of density vs. depth was constructed. Additionally, the disks were cut into two halves vertically and the density variation across the samples in plane was calculated.

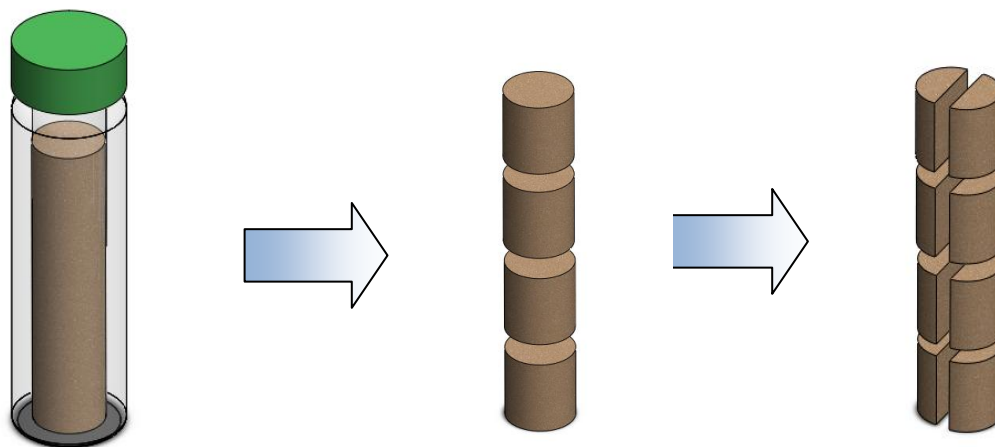


Figure 11: Depiction of samples created for density testing.

Results and Discussion

The vial holder is currently built. It matches the dimensions specifications and holds 16 0.97 in vials. Additionally, a suitable water-tank has been found and purchased for under \$10. Additional component prices are given in Appendix B – Relevant Figures, Table 7. Four emulsions have been created thus far (Table 3). describes the components of these emulsions and the average temperature at which the components were mixed. More details are given in Appendix B – Relevant Figures, Table 6. All fractions were calculated by weight, not volume. Because these samples were created while searching for the optimal procedure, the amounts of gelatin in them are different. The combination of gelatin, formalin, and temperature used for the 17.08% fat sample was found to be optimal for further emulsion creation.

Table 3: Final concentrations of emulsion components.

Fat fraction (percent by weight)	Gelatin (percent by weight)	NaN3 (g)	Soap (mL)	Formalin (mL)	Temperature (F)
3.76%	0.1241	0.9	0.5	0.3	120
4.82%	0.1584	0.9	0.5	0.5	120
7.56%	0.1968	0.9	0.5	0.4	170
17.08%	0.1961	0.9	0.5	0.3	140

Testing Results and Discussion

The IDEAL image of the emulsions is shown in Figure 12. The fat fractions measured in the image are given in Table 4. Pure water and pure fat were quantified as 1.4% and 104.5%, respectively. The latter discrepancy, at least in part, is due to the fact that the IDEAL was set to identify fat based on a single major chemical shift peak. The IDEAL can be set up to perform quantification using more than one peak of the safflower oil signal as this oil's peaks and chemical shifts are known. This can be done during the calibration procedure if the scanner is reset to the original peak settings subsequently. As can be seen from Figure 13, the pure oil and the oil with soap and formalin emulsions were negligibly different. Thus, the use of these components in other emulsions should not interfere with the measurements.

Table 4: Expected and obtained fat fractions readings from the IDEAL Procedure. *Sample H separated into water and oil layers during the scan.

Sample	Gelatin	Actual fat fraction	Measured fat fraction
A		0%	1.4%
B	•	4.82%	2.6%
C	•	3.76%	3.1%
D	•	7.56%	5%
E	•	17.08%	10.2%
F		100%	104.5%
G		100%	105.2%
H*		15%	0.4%

When quantifying un-fixated emulsions at 0%, 100% and 100% with soap and formalin emulsions, the measured fat fractions were higher than the actual values (Figure 13). For all samples containing gelatin, the measured fat fraction was lower (Figure 15). This is likely due to the fact that the signal from gelatin resembles that of water. Also note that the

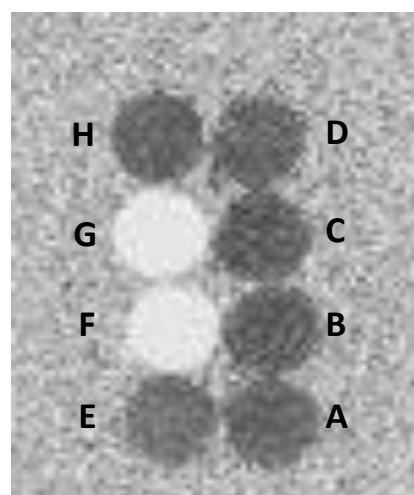


Figure 12: IDEAL fat fraction image of the fixated (B-E) and unfixated (A, F-H) emulsions.

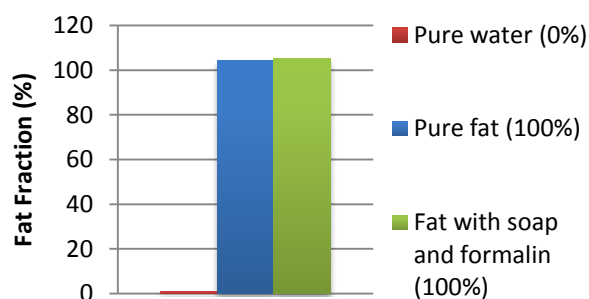


Figure 13: Measured fat fractions of pure water, pure fat, and fat with formalin and soap.

amount of gelatin in each sample increases with increasing fat fraction (Figure 14). This causes a discrepancy between the actual and measured fat fraction, thus final emulsions should contain consistent amounts of gelatin.

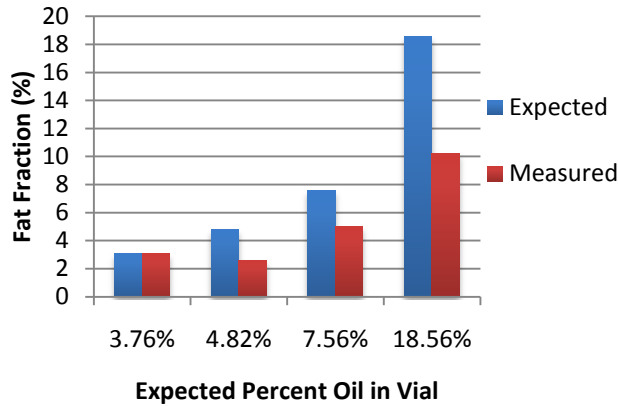


Figure 15: Measured vs. expected fat fractions for fixated emulsions. The amount of gelatin, as well as the discrepancy, increases from left to right.

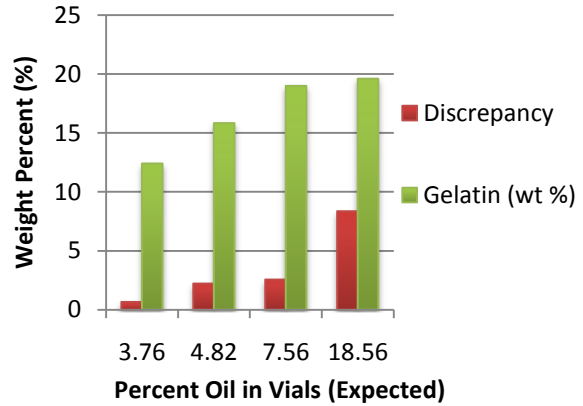


Figure 14: Weight percent of gelatin in the four finished emulsions and the discrepancy of measured vs. expected weight percent of oil.

The homogeneity of the emulsions in terms of density was also tested. The density variation top-to-bottom is presented in Figure 16. Surprisingly, the density decreases towards the bottom of the sample. This is attributed to the fact that when the emulsions are made, the lowest density is at the top. Subsequently, formalin is added, and they are poured into the vials. The lowest density material is poured first, and the emulsion solidifies before the densities can become even. While the density gradient is not large, it may be a cause for concern as the density variation is believed to be due to the difference in fat-water fraction. Thus, imaging the sample in different planes would give varying results. A better mixing procedure in the vertical direction may be able to reduce this effect.

Figure 17 shows the variation of density across one plane in the sample. Though a gradient can be observed, the sample size is too small to draw conclusions about its accuracy.

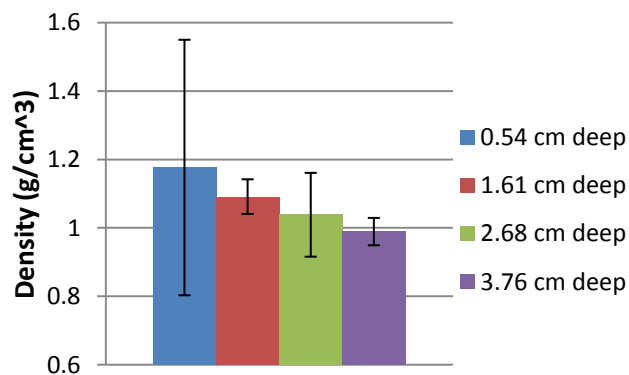


Figure 16: Density variation in emulsions from top to bottom. Error bars represent ± 1 standard deviation in either direction.

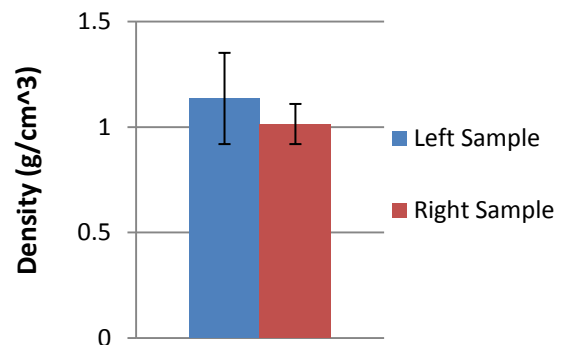


Figure 17: Density of an emulsion throughout its bulk across its width; Error given in ± 1 standard deviation.

Future Work

Some work remains to be done on this phantom before it is suitable for use by the client. A basic timeline can be laid out for future work on the phantom during the next semester:



Essentially, the work that remains to be done involves further testing of the phantom, creation of 16 emulsions that are ready for client use, incorporating any mechanical features into the phantom that would increase ease of use, and solving other minor problems that arose with the

phantom this semester. To create more homogeneous emulsions, better chemical mixing techniques will be used. The noted signal differences caused by the presence of gelatin will be quantified and corrected for. Once the previous steps have been completed, all sixteen emulsions that are ready for client use will then be created. Testing of the phantom's performance will then begin. This will involve ensuring the repeatability of the phantom's behavior as well as its longevity. If during the course of this testing changes to the mechanical design are deemed necessary, they will also be completed at this time. The end goal is creation of a phantom that the client can use by the end of the Spring 2010 semester.

Conclusion

This semester, an MRI phantom was created to calibrate the client's IDEAL fat quantification procedure. The mechanical structure and the procedure for creating the chemical components of a phantom were developed. The prototype design consists of an UHMWPE vial holder that has capacity for 16 different samples. These components are submerged in water to avoid air-to-sample interfaces that may interfere with the MR signal of the phantom. The samples, which attempt to mimic the signal of fat within the liver, are safflower oil-in-water emulsions that are fixated with bovine gelatin type B. Different liver fat concentrations are represented through variation of the fraction of oil relative to water. Preliminary testing suggests that the phantom will function well with the client's IDEAL procedure. Though future work is necessary, the phantom will hopefully be functional by May 2010.

Bibliography

- Albright, Ann L., and Judith S. Stern. "Adipose Tissue." *Encyclopedia of Sports Medicine*, 1998.
- Amazon.com. *Amazon.com*. 2009. http://www.amazon.com/Lock-Shrinkwrap-Rectangular-Value-Storage/dp/B001AS8FK8/ref=sr_1_1?ie=UTF8&qid=1257827670&sr=8-1 (accessed November 11, 2009).
- Ataseven, H, M H Yildirim, and M Yalniz. "Correlation between calibrated computerized tomographic findings and histopathologic grade/stage in non-alcoholic steatohepatitis." *Journal of Hepatology*, Vol 38, 2003: A3842.
- Bao, Lei, Wei Yang, and Xuan Mao. "Agar/collagen membrane as skin dressing for wounds." *Biomed. Mater.*, 2008.
- Barak, AJ, HC Beckenauer, and DJ Tuma. "Dietary betaine promotes generation of hepatic s-adenosylmethionine and protects the liver from ethanol-induced fatty infiltration." *Alcohol Clin Exp Res* 17, 1993: 552-555.
- Belechinger, JC, EL Madsen, and GR Frank. "Tissue-mimicking gelatin-agar gels for use in magnetic resonance imaging phantoms." *Medical Physics*, 1988: Vol 15, No. 4. 629-636.
- Blechinger, J. C., E. L. Madsen, and G. R. Frank. "Tissue-mimicking gelatin-agar for use in magnetic resonance imaging phantoms." *Medical Physics*, 1988: 629-636.
- Block, Dr. Walter, and Catherine Hines, interview by Bogdan Dzyubak, Joe Helfenberger and Matt Parlato. *Project Meeting* (October 7, 2009).
- Boedeker. *Guide to Plastics Machining*. . 2009. <http://www.boedeker.com/fabtip.htm> (accessed December 7, 2009).
- Chang, Jerry S., Taouli Bachir, Nouha Salibi, Deanna G. Chin, Vivian S. Lee, and Elizabeth M. Hecht. "Opposed-Phase MRI for Fat Quantification in Fat-Water Phantoms with 1H MR Spectroscopy to Resolve Ambiguity of Fat or Water Dominance." *American Journal of Roentgenology*, 2006: 187:103-106.
- Christie, Dr. William W. *The Lipid Library*. November 27, 2009. <http://www.lipidlibrary.co.uk> (accessed September 24, 2009).
- Diamond, Joy, Vallipuram R Thava, and Brian B Scott. "Diagnosis of fatty liver disease: is biopsy necessary?" *European Journal of Gastroenterology & Hepatology*, 2003: Volume 15 - Issue 5 - pp 539-543.
- Diehl, Anna Mae, and Brent Tetre. *National Digestive Diseases Information Clearinghouse: Nonalcoholic Steatohepatitis*. November 2006. <http://digestive.niddk.nih.gov/ddiseases/pubs/nash/> (accessed October 30, 2009).
- Dominquez, LJ, MR Tagliamonte, and MB Ballibigto. "Effects of vitamin E and glutathione on glucose metabolism: role of magnesium." *Hypertension* 34, 2005: 1002-1006.

Edens, Alexander. *Adipose Tissue Photo*. <http://www.hartnell.cc.ca.us/faculty/aedens/Bio6L/tissue-adiposeB.jpg> (accessed October 30, 2009).

Erasmus, Udo. "Fat content and fatty acid composition of seed oils." *CureZone.com*. 2009. <http://curezone.com/foods/fatspercent.asp> (accessed October 1, 2009).

Ferenci, P, N Tozun, and N Avsar. "Diagnosis of Non Alcoholic Fatty Liver Disease." *EASL President's Premeeting Syllabus*. 2003. 33-40.

Fraenkel-Conrat, Heinz, and Dale Mecham. "The reaction of formaldehyde with proteins." *Journal of Biological Chemistry*, 1948.

Frank, Gary, interview by Bogdan Dzyubak, Nick Balge, Matt Parlato and Joe Helfenberger. (October 2, 2009).

Gerbig, Steve. *Relative Dimensional Change of Various Nylon Products Due to Moisture Absorption*. 2009. http://www.ides.com/articles/polyamide_moisture_absorption.asp (accessed December 7, 2009).

Hannesson, P. H., N.O. Wallengren, K. Lyttkens, T. Melin, S. Brockstedt, and E. Stahlberg. "Magnetic resonance imaging with signal-intensity measurements in diffuse liver disease." *European Radiology*, 1995: 5,626-629.

Heiken, J. P., J. K. Lee, and W. T. and Dixon. "Fatty infiltration of the liver: evaluation by proton spectroscopic imaging." *Radiology*, 1985: 707-710.

Hines, Catherine, interview by Joe Helfenberger, and Bogdan Dzyubak Matthew Parlato. *Research Assitant, UW-Madison Radiology Department* (October 7, 2009).

Koka, Rene´ D., Marieke M. de Vriesa, Arend Heerschabp, and Paul P. and van den Berga. "Absence of harmful effects of magnetic resonance exposure at 1.5 T in utero during the third trimester of pregnancy: a follow-up study." *Magnetic Resonance Imaging*, 2004: 851-854.

Kokatmur, M. G., M. C. Oalman, W. D. Johnson, G. T. Malcom, and J. P and Strong. "Fatty acid composition of human adipose tissue from two anatomical sites in a biracial community." *The American Journal of Clinical Nutrition*, 1979: 2198-2205.

Marchesini, G, and G Forlani. "NASH: From liver diseases to metabolic disorders and back to clinical hepatology." *Hepatology* 35, 2002: 497-499.

Matsunaga, Sayoko, et al. "Dual Double-gradient-echo MRI for Liver Fat Content Analysis." *Medical Imaging and Information Sciences*, 2006: Vol. 23 No. 1 pp.8-10.

Menesson, Nicolas, et al. "Liver Steatosis Quantification Using Magnetic Resonance Imaging: A Prospective Comparative Study With Liver Biopsy." *Journal of Computer Assisted Tomography*, 2009: Volume 33 - Issue 5 - pp 672-677.

- Mott, et al. *Artificial Environments for Growing Bacteria*. . January 5, 2005.
www.woodrow.org/teachers/esi/2002/Biology/Projects/lab_skills/ls5/ (accessed December 6, 2009).
- Muraca, M, and R Dianzani. "Vitamin E dietary supplementation inhibits transforming growth factor beta-1 gene expression in rat liver." *FEBS Lett, No. 308*, 1992: 267-270.
- Occupational Safety and Health Administration. *Back Disorders and Injuries*. January 1, 2009.
http://www.osha.gov/dts/osta/otm/otm_vii/otm_vii_1.html.
- Ogden, CL, CD Fryar, MD Carrol, and KM Flegal. "Mean Body Weight, height and body mass index of United States from 1960-2002." 2004.
- Patrick, Lyn. "Nonalcoholic fatty liver disease: relationship to insulin sensitivity and oxidative stress. Treatment approaches using vitamin E, magnesium, and betaine." *Fatty Liver Alternative Medicine Review*, 2002.
- Pessayre, D, A Bearson, B Fromenty, and A Mansour. "Mitochondria in steatohepatitis." *Semin Liver Dis* 21, 2001: 57-69.
- Plastics*. 2009. <http://www.mcmaster.com/#plastics/=4tkv52> (accessed December 6, 2009).
- Porath, Jerker Olof, and Jan-Christer Janson. Stabilized agar product and method for its stabilization. US Patent 3959251. May 25, 1976.
- Powell, E. E., W. G. Cooksley, and R. Hanson. "The natural history of nonalcoholic steatohepatitis: a follow-up study of 42 patients for up to 21 years." *Hepatology, No 11*, 1990: 74-80.
- Reeder, Dr. Scott, interview by Matthew Parlato. *Personal Communication* (October 9, 2009).
- Reeder, Dr. Scott, interview by Matthew Parlato. *Personal Communication* (October 8, 2009).
- Reeder, Dr. Scott, interview by Bogdan and Parlato, Matthew Dzyubak. *Project Meeting* (September 17, 2009).
- Reeder, Dr. Scott, interview by Matt Parlato. *Relevant Fat Concentrations* (October 8, 2009).
- Saeian, K, K Curro, and DG Binion. "Plasma total homocysteine levels are higher in nonalcoholic steatohepatitis." *Hepatology* 30, 1999: 436A.
- SAFC. "ProClin® Preservatives for In Vitro Diagnostic Materials: Efficacy vs. Thimerosal and Sodium Azide." 2009.
- Samsheer, KS, D Farell, S Campbell, N Kochar, and F George. "Clinicopathological features and predictors of fibrosis in non alcoholic fatty liver disease (NAFLD) patients in the south west of England." *Journal of Hepatology, Vol 38*, 2003: A4177.

Schenck, J. F. "The role of magnetic susceptibility in magnetic resonance imaging: MRI magnetic compatibility of the first and second kinds." *Medical Physics*, 1996: 815-843.

Sigma-Aldrich. *Agar Powder*. 2009.

http://www.sigmaaldrich.com/catalog/ProductDetail.do?lang=en&N4=318078|ALDRICH&N5=SEARCH_CONCAT_PNO|BRAND_KEY&F=SPEC (accessed December 2009, 2009).

Song, H. K., A. C. Wright, R. L. Wolf, and F. W. and Wehrli. *Comparison of 2- and 3-Point Dixon Techniques in RF- and Readout-Shifted FSE Sequences*. Pennsylvania.

VWR International. *Gelatin, Type B*. 2009.

https://www.vwrsp.com/catalog/product/index.cgi?catalog_number=MKH21959&inE=1&highlight=MKH21959 (accessed December 7, 2009).

WebMD. *Digestive Disorders Health Center: Alanine Aminotransferase (ALT)*. January 2, 2008.

<http://www.webmd.com/digestive-disorders/alanine-aminotransferase-alt> (accessed October 30, 2009).

Wikimedia: *Human Liver*. June 2, 2006.

http://upload.wikimedia.org/wikipedia/commons/f/fc/Human_liver.jpg (accessed October 30, 2009).

Wikimedia: *Non-alcoholic fatty liver disease1*. September 11, 2009.

http://en.wikipedia.org/wiki/File:Non-alcoholic_fatty_liver_disease1.jpg (accessed October 30, 2009).

Yoneda, M, K Fujita, M Inamori, and A Nakajima. "Transient elastography in patients with non-alcoholic fatty liver disease (NAFLD)." *Gut* 56, 2007 : 1330-1331.

Appendix A – Product Design Specifications

MRI Phantom

Bogdan Dzyubak – Team Leader
Joe Helfenberger – BSAC
Nick Balge -- BWIG
Matt Parlato -- Communicator

Clients:

Dr. Scott B Reeder
Medical Physics and Radiology
Phone: (608) 265-9964
Email: sb.reeder@hosp.wisc.edu

Dr. Walter F Block
Biomedical Engineering and Electrical Engineering
Phone: (608) 265-9686
Email: wfblock@wisc.edu

Advisor:

Dr. Naomi C Chesler
Dept. of Biomedical Engineering
2146 Engineering Centers Building
1550 Engineering Dr
Madison, WI 53706
Phone: (608) 265-8920
(608) 263-4660
Email: chesler@enr.wisc.edu

Function:

The goal of this project is to develop an MRI phantom for the calibration and testing of MRI techniques that quantify fat. This phantom will be used as a quality control mechanism for sites that wish to utilize MRI to quantify fat. Quantities of fat used within the phantom are accurate to within $\pm 0.3\%$, and their MR signal will not change over a number of years.

Client Requirements:

- **Accuracy:** The concentrations of fat within the phantom must be accurate to within $\pm 0.3\%$. The method employed to create the fat and water emulsions must yield reproducible results.
- **MRI Constraints:**
 - No magnetic materials can be used for the construction of this device.
 - The phantom must be of appropriate size to fit easily within a standard single channel MRI head coil.
 - The materials and chemicals, such as preservatives or emulsifiers, must not interfere significantly with the oil/water signal.
 - Air-to-sample interfaces must be minimized.

- **Range of Fat Concentrations:** The phantom must represent physiological fat concentrations for different organs in the body. Samples will need to exist surrounding 5% and 90% fat, as well as cover the range between 5% and 50% fat.
- **Shelf Life:** The phantom must have a shelf life of at least three years.

Design Requirements:

1. Physical and Operational Characteristics

- a. *Performance requirements:* The concentrations of fat within the phantom must be accurate to within $\pm 0.3\%$ and be reproducible. These values should not change for the specified lifetime of the phantom. Also, as air is paramagnetic (i.e. interferes with MR imaging), air-to-sample interfaces must be minimized within the phantom.
 - I. *Fat Concentrations:* Concentrations must be physiologically relevant. They must specifically surround the 5% concentration as this is recognized as the diagnostic cutoff for Fatty Liver Disease.
- b. *Safety:* Materials used in the phantom should be non-toxic, non-caustic, non-allergenic, chemically stable, and non-magnetic.
- c. *Life in Service:* The phantom should yield consistent measurements for 3 years. It must withstand standard hospital cleaning procedures such as washing with isopropyl alcohol or similar agents.
- d. *Shelf Life:* The conditions of use are not damaging to the phantom so shelf life should be equivalent to life in service.
- e. *Operating Environment:* Strong magnetic fields of over 3 T may be used. These should not be damaging to the phantom, negatively affect its performance, or cause the phantom to become potentially harmful.
- f. *Ergonomics:* Phantom should be easy to handle and transport by one person.
- g. *Size:* Phantom must fit within a standard MRI head coil (27 cm diameter by 42 cm depth).
- h. *Weight:* It should weigh less than 20 lbs so that one person can easily handle/transport it.
- i. *Materials:* The phantom must consist of non-magnetic materials, and none of its components should interfere with fat quantification. Materials should also be transparent or translucent to allow for the user to easily detect damage to internal phantom components.
 - I. *Fat Simulation Materials:* Due to sanitation and degradation concerns, the use of actual fat in this phantom will not be feasible. Instead, other materials displaying similar imaging characteristics need to be used.

2. Production Characteristics

- a. *Quantity*: Currently, the client only requires one phantom.
- b. *Target Product Cost*: The phantom prototype should cost less than \$300 to produce. Production on a larger scale would significantly reduce cost.

3. Miscellaneous

- a. *Standards and Specifications*: Oil/water solutions must be accurate and reproducible in large quantities. Dimensions for the phantom also must be standardized for potential mass production.
- b. *Customer*: The phantom should be easy to use so that potential customers are not discouraged.
- c. *Patient-related concerns*: The phantom will be used in the same scanner as patients. Therefore, the phantom materials must be non-toxic, non-caustic, non-allergenic, and chemically stable. The phantom must not leave residues upon surfaces it comes into contact with.
- d. *Competition*: Other quality control and research phantoms exist but few deal with fat quantification. Simpler designs can be used as an alternative, however, their accuracy cannot be guaranteed.

Appendix B – Relevant Figures

Table 5: Projected emulsion concentrations.

Volume (oil, water)(mL)*	50	50	50	50	50	50	50	50	50	50	50
Weight (oil, water)(g)*	50	49.9	49.8	49.8	49.7	49.7	49.6	49.4	49.2	49	48.7

Wt Percent of Fat (%)*	0	3	4	5	6	7	10	15	20	25	30
Wt Percent Water (%)*	100	97	96	95	94	93	90	85	80	75	70
Weight Fat (g)	0	1.5	1.99	2.49	2.98	3.48	4.96	7.4	9.83	12.2	14.6
Weight of water (g)	50	48.4	47.8	47.3	46.8	46.2	44.6	42	39.3	36.7	34.1
Volume Oil and H ₂ O (mL)*	100	100	100	100	101	101	101	101	102	102	103
Emulsifier (mL) ***	0.5	0.5	0.5	0.5	0.5	0.5	0.5	0.5	0.5	0.5	0.5
Animal Hide Gel (g) ****	7.47	8.8	7.45	9.48	7.6	12.4	12.4	12.3	7.51	7.48	7.45
Weight % of Gel**	13	15	13	16	13.3	20	20	20	13.3	13.3	13.3
Formalin (g) ****	0.43	0.43	0.42	0.44	0.42	0.46	0.46	0.46	0.42	0.42	0.42
Weight % of formalin**	0.74	0.74	0.74	0.74	0.74	0.74	0.74	0.74	0.74	0.74	0.74
% Oil by Volume**	0	2.98	4.03	4.94	6.02	6.72	9.58	14.3	19.9	24.7	29.6
Formalin (mL) to deliver	0.39	0.4	0.39	0.41	0.39	0.43	0.42	0.42	0.39	0.39	0.39

Volume (oil, water)(mL)*	50	50	50	50	50
Weight (oil, water)(g)*	48.3	47.9	46.4	46.3	46.2

Wt Percent of Fat (%)*	40	50	90	92.5	95
Wt Percent Water (%)*	60	50	10	7.5	5
Weight Fat (g)	19.3	24	41.8	42.9	43.9
Weight of water (g)	29	24	4.64	3.47	2.31
Volume Oil and H ₂ O (mL)*	103	104	108	108	108
Emulsifier (mL) ***	0.5	0.5	0.5	0.5	0.5
Animal Hide Gel (g) ****	7.38	7.32	7.09	7.08	7.06
Weight % of Gel**	13.3	13.3	13.3	13.3	13.3
Formalin (g) ****	0.41	0.41	0.4	0.4	0.39
Weight % of formalin**	0.74	0.74	0.74	0.74	0.74
% Oil by Volume**	39.2	48.6	85.1	87.3	89.5
Formalin (mL) to deliver	0.38	0.38	0.37	0.37	0.37

* Calculated including oil and water.

** Calculated including oil, water and gelatin.

*** Emulsifier was set to 1% by volume of fat and water

**** Target values are a function of input values entered as wt percent

Density of Safflower Oil is 0.921 g/cm³Density of formalin is 1.08 g/cm³

Weight of Oil/water formula =

$$\left(1 + \frac{\% \text{ fat}}{\% \text{ water}}\right) * \frac{\text{total mL}}{1.086 * \frac{\% \text{ fat}}{\% \text{ water}} + 1}$$

Table 6: Component amounts, temperatures and crosslinking times that were used for each completed emulsion.

Percent of Fat	3%	4%	7%	15%
Weight of Water (g)	48.3672	47.1974	46.1890	42.0421
Weight of Fat (g)	1.8200	2.2754	3.4919	7.1800
Weight of Gelatin (g)	7.2573	9.4879	12.4280	12.2277
Formalin (mL)	0.4000	0.3000	0.4000	0.3000
Sodium Azide (g)	0.0987	0.1102	0.0960	0.0888
Ivory Soap (mL)	0.5000	0.5000	0.5000	0.5000
Total Weight (g)	58.4752	59.8949	63.1369	62.3626
<u>Temperature (degrees F)</u>				
High (after Gelatin was Liquefied)	190.0	162.0	168.0	148.0
Low (before formalin was added)	117.0	113.0	165.0	128.0

Time between formalin addition and pouring	20.0	15.0	5.0	1.5
--	------	------	-----	-----

Ratio (%) of Fat/Water by weight	0.0376	0.0482	0.0756	0.1708
Ratio (%) of Fat/Water by volume*	0.0409	0.0524	0.0822	0.1856
Weight % Gelatin based on total**	0.1241	0.1584	0.1968	0.1961
Conc. of Sodium Azide (mM) ***	25.9523	28.2729	23.3254	21.7280
Weight % of Formalin	0.0074	0.0054	0.0068	0.0052

Table 7: Price breakdown of components purchased for phantom prototype.

<u>Company</u>	<u>Item Name</u>	<u>Dimensions</u>	<u>Item Number</u>	<u>Quantity</u>	<u>Price</u>
Fisher Scientific	Formaldehyde (37% Aq Formalin)	500 mL	RSOF0010500	1	\$23.01
Amazon.com	School Supply Case	6.5" x 9.2" x 3.7"	B001AS8FK8	1	\$7.99
McMaster-Carr	UHMWPE	4"X6"X6"	8752K972	1	\$43.75
McMaster-Carr	30 mL Clear Glass Vials	0.98" outer diameter, 3.75" outer length	4417T47	7 Cases	\$83.72
Amazon.com	Ivory Hand Soap	16 oz	B000FK5TDS	1	\$8.00
VWR Scientific	Animal Hide Gel	100 grams	100504-032	1	\$26.71
Amazon.com	Safflower Oil	8.5 fl oz	B00014FYV0	1	\$6.99
				Total Cost	\$200.17

Appendix C – Weight Limit Calculations

According to the US Department of Labor’s division of Occupational Safety and Health Administration, the recommended weight limit of an object is a function of several elements, including:

- Horizontal Multiplier (HM): Horizontal distance from person’s center of gravity
- Vertical Multiplier (VM): The height to which the object is lifted to
- Distance Multiplier (DM): The total distance over which the object is lifted over
- Asymmetric Multiplier (AM): Based on the angle of torso twist undergone during lifting
- Frequency Multiplier (FM): Taking into consideration how many times the object is lifted
- Coupling Multiplier (CM): A multiplier factor based on how easy the object can be lifted

The recommended weight limit is then a function of a load constant and the multiplication of each of these values (Occupational Safety and Health Administration 2009).

$$\begin{aligned} \text{Recommended weight limit} \\ = \text{Load Constant (51 lbs)} \cdot (HM) \cdot (VM) \cdot (DM) \cdot (AM) \cdot (FM) \cdot (CM) \end{aligned}$$

Estimation of Multiplier Values:

The horizontal multiplier is given by $10/H$, where H is the horizontal distance the object rests from the person’s center of mass. It was estimated using forearm data and adding 2 standard deviations for the average value so that 95 percent of forearm values are included, with H of 13.1 inches (Ogden, et al. 2004).

$$HM = \frac{10 \text{ in}}{13.1 \text{ in}} = 0.75$$

The vertical multiplier is given as $(1 - 0.0075 \cdot |V - 30|)$, where V is the vertical distance to the hands in inches. This was calculated by using survey information of US adults from 1960-2002 using an anthropometric data table to find the average distance from the ground to the elbow (Ogden, et al. 2004). Two standard deviations were added to encompass 95% of vertical heights.

$$VM = (1 - 0.0075 \text{ in}^{-1} \cdot |46.62 \text{ in} - 30 \text{ in}|) = 0.87535$$

The distance multiplier was estimated using a worst case scenario: the phantom is stored in a lower cabinet close to the ground. The value of DM is defined as $0.82 + \frac{1.8}{D}$, where D is the total distance traveled. This was estimated by $(V - 3 \text{ in}) = 43.62 \text{ in}$.

$$DM = 0.82 + \frac{1.8 \text{ in}}{43.62 \text{ in}} = 0.86$$

The asymmetric multiplier was also estimated in a worst case scenario: the phantom is stored such that a person must twist their torso to reach it. A reasonable angle was determined to be 45°, but 70° was used for a conservative estimate. The multiplier value is defined as $(1 - (0.0032 \cdot A))$.

$$AM = (1 - 0.0032 \cdot 70^\circ) = 0.776$$

The frequency multiplier and coupling multipliers are obtained from table on the Occupational Safety and Health Administration's website (Occupational Safety and Health Administration 2009). This led to selection values of FM of 1.00 due to the low frequency of movement and CM of 1.00 based on "good" or "fair" handling design.

$$\text{Recommended weight limit} = 51 \text{ lbs} \cdot 0.75 \cdot 0.875 \cdot 0.86 \cdot 0.776 \cdot 1 \cdot 1 = 22.3 \text{ lbs}$$

The total multiplication of these values gave a recommended weight limit of 22.3 lbs. This confirms our set weight limit of 20 lbs in the product design specifications.